

Influence of Chain Structure on the Miscibility of Poly(vinylidene fluoride) with Poly(methyl acrylate)

Pralay Maiti and Arun K. Nandi*

Polymer Science Unit, Indian Association for the Cultivation of Science, Jadavpur, Calcutta 700 032, India

Received March 20, 1995; Revised Manuscript Received July 20, 1995*

ABSTRACT: The blending ability of poly(vinylidene fluoride) (PVF₂) depends on the head-to-head (H–H) defect structure present in the chain. With increasing H–H defect content, the lower critical solution temperatures (LCST) of PVF₂/PMA blends decrease. This has been explained from the polymer–polymer interaction parameter (χ_{12}) values measured from the equilibrium melting point (T_m°) depression of the α phase of PVF₂. A critical analysis on the method of measuring the equilibrium melting point from the Hoffman–Weeks plot has been done. For Hoffman–Weeks plots the T_m (melting point) should be determined for the same and low level of crystallinity at each T_c (crystallization temperature) to obtain correct results. If T_m is counted for the same time of crystallization at each T_c , erroneous results are obtained. Extrapolation of the $T_m - T_a$ (T_a = annealing temperature) plot to the $T_m = T_a$ line also yields the correct T_m° . χ_{12} values are determined with all these T_m° s, and it has been observed that the annealing method and the same crystallinity method yield almost same value of χ_{12} , which can explain the LCST phase diagram of PVF₂ blends. Annealing results yield that PVF₂ up to 24 mol % H–H defect concentration would be miscible with PMA. χ_{12} measured from T_m° s of the same time of crystallization and from the apparent melting points of PVF₂ blends yield incorrect results.

Introduction

During the past two decades poly(vinylidene fluoride) (PVF₂) blends have been widely studied.^{1–8} PVF₂ is not completely isoregic and has different amounts of head-to-head (H–H) defects.⁹ In this paper we report the influence of H–H defect content on the blending ability of PVF₂. The blending ability of a polymer is usually directed by the polymer (1)–polymer (2) interaction parameter (χ_{12}), which is defined as¹⁰

$$\chi_{12} = \frac{\mu_1^R}{RT\phi_2^2} \quad (1)$$

where μ_1^R is the residual chemical potential of component 1 and is independent of the combinatorial entropy of mixing. ϕ_2 is the volume fraction of component 2. The χ_{12} can be measured by a number of different procedures.¹¹ For blends of crystalline polymers with amorphous polymers, the melting point depression method is usually applied. Nishi and Wang¹² derived an expression for the depression of the melting point from Scott's¹³ treatment on the thermodynamics of mixing of two polymers

$$\frac{1}{T_{mb}^\circ} - \frac{1}{T_m^\circ} = - \frac{RV_c}{\Delta H_u V_a} \phi_a^2 \chi_{12} \quad (2)$$

where T_{mb}° and T_m° are the equilibrium melting points of the blend and that of the pure polymer, respectively. V_c and V_a are the molar volumes of the repeating units of the crystalline polymer and the amorphous polymer, respectively. ϕ_a is the volume fraction of the amorphous polymer, and ΔH_u is the enthalpy of fusion per mole of the repeating unit of the crystalline component. For the two polymers to be miscible, the χ_{12} must be smaller than the critical value¹³ of χ_{12}

$$\chi_{12}^C = \frac{1}{2} \left[\frac{1}{r_1^{1/2}} + \frac{1}{r_2^{1/2}} \right]^2 \quad (3)$$

where r_1 and r_2 are essentially the number of segments of component 1 and component 2, respectively. For polymer–polymer systems, the χ_{12}^C is very close to zero, and, therefore, for the polymers to be miscible the χ_{12} should be negative and only then there is a reasonable depression of the equilibrium melting point of the blend. The extent of miscibility is directly manifested in the phase diagrams of the blends. Miscible polymer–polymer systems usually show demixing when heated (lower critical solution temperature (LCST)).¹¹ This behavior arises due to the rapid increase of the interactional part of χ_{12} with temperature,¹⁴ and when χ_{12} becomes larger than χ_{12}^C , phase separation occurs. Thus, LCST measurement would help to understand the blending ability of the two polymers. However, the LCST also depends on molecular weight,¹¹ and care must be taken to arrive at any definite conclusion regarding this matter.

Therefore, to find the extent of miscibility an accurate determination of χ_{12} is necessary and to determine χ_{12} an accurate value of equilibrium melting point is required.¹⁵ There are three different methods^{16,17} for determining the equilibrium melting point: (I) extrapolation of the $T_m - T_c$ plot to the $T_m = T_c$ line (Hoffman–Weeks plot), (II) extrapolation of the $T_m - T_a$ plot to the $T_m = T_a$ line, and (III) extrapolation of the $T_m - 1/l$ plot to the $l = \alpha$ line, where T_m , T_c , and T_a are the melting, crystallization, and annealing temperatures, respectively, and l is the lamellar thickness. Of these three methods, the first two methods are usually applied frequently because of easier instrumentation. The Hoffman–Weeks equation for the determination of the equilibrium melting point is

$$T_m = T_m^\circ [1 - (1/\gamma)] + T_c/\gamma \quad (4)$$

where γ is the thickening ratio.^{16,17} Determination of the correct T_m at a given T_c with eq 4 is difficult,¹⁸ and in applying the first method, care must be taken to

* Abstract published in *Advance ACS Abstracts*, September 1, 1995.

Table 1. Characteristics of PVF₂, VF₂-VF₄ Copolymers, and Poly(methyl acrylate) Samples

sample	$\bar{M}_w \times 10^{-5}$	PDI	H-H defect (mol %)	crystallinity ^a	mp (°C)
KF-1000 (KF)	4.28	1.47	3.5	57.3	176.6
KY-201 (KY)	7.36	2.04	5.31	49.1	164.3
KFE	5.08	1.43	3.75	53.4	175.0
KYA	6.52	1.77	5.06	49.0	165.2
KYD	7.46	2.45	5.64	46.2	161.6
Cop-1	1.97	2.07	15.8	27.7	150.8
Cop-2	3.23	2.63	21.3	19.1	138.5
Cop-3	4.59	2.45	27.6	23.9	132.1
PMAU	2.57	1.62			
PMA2	4.04	1.56			

^a Cop-1 and Cop-2 were crystallized at 120 °C, Cop-3 was crystallized at 110 °C, and the other samples were crystallized at 144 °C for 24 h.

monitor the correct T_m at each T_c .¹⁹ The correct procedure for monitoring T_m for the Hoffman-Weeks plot is to consider the melting point at the same crystallinity for each T_c for a very low level of crystallinity.²⁰ If T_m is monitored at the same time of crystallization at each T_c , the development of different amounts of crystallinity and also different amounts of thickening violates the postulates of this extrapolation.¹⁹ In the determination of T_m° s of PVF₂ fractions, we noticed earlier that T_m s at the same time of crystallization yield very low values of T_m because of thickening.¹⁹ In the case of blends, here we also judged the determination of T_m° on the same time basis and hence χ_{12} , as most workers used to determine T_m° and χ_{12} by this method.

Experimental Section

Materials. Two commercial poly(vinylidene fluoride) (PVF₂) samples and three fractions were used. Three vinylidene fluoride-tetrafluoroethylene (VF₂-VF₄) copolymers were also used. The characteristics of these samples are presented in Table 1. The PVF₂ fractions (KFE, KYA, and KYD) were prepared from the KF and KY PVF₂ samples and were characterized using a procedure published earlier.¹⁹ The fractions were chosen with a closer match of molecular weight but having a significant difference in defect concentration. H-H defects were measured by ¹⁹F NMR spectroscopy, and the molecular weights were determined by GPC.²¹ The unfractionated PMA sample (PMAU) was used to make blends with the whole PVF₂ sample, and the second fraction of PMA (PMA2) was used to make blends with PVF₂ fractions. The PMA fraction was prepared by the liquid-liquid phase separation technique using the benzene/methanol system. The fractionated samples of PVF₂ were used to observe any effect of structural polydispersity on its interaction with poly(methyl acrylate). The melting points and the crystallinities presented in Table 1 for the PVF₂ samples and those of the VF₂-VF₄ copolymers were measured using procedures described earlier.^{19,21} Blends of varying compositions were prepared using a procedure described earlier.⁷

The LCSTs of the systems were measured by the light scattering method using an apparatus fabricated in our laboratory.²² The heating rate during the scan was monitored to be 2 °C/min. The cloud point was taken as the onset temperature of the change in the intensity of light during heating. Each experiment was repeated three times, and the average temperature was taken as the cloud point.

For measurement of the equilibrium melting temperatures, isothermal crystallizations were carried out on a DSC-7 (Perkin-Elmer) equipped with a 3700 data station. The samples were initially melted at 227 °C for 5 min and then quenched at the rate of 200 °C/min to the predetermined isothermal temperature. Crystallizations were done for different times at different temperatures. The samples were melted at the heating rate of 10 °C/min from the isothermal

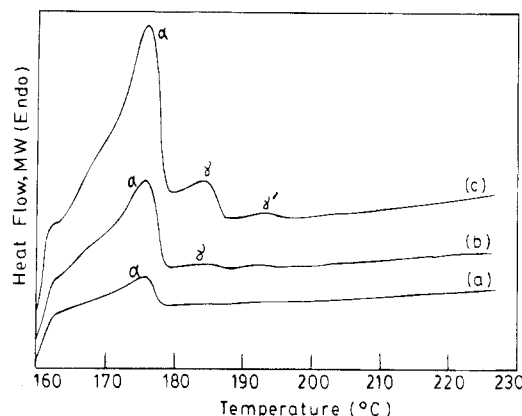


Figure 1. Melting endotherms of KFE/PMA2 ($w_{\text{PVF}_2} = 0.75$) blend crystallized at 160 °C for different times: (a) 4, (b) 9, and (c) 20 h.

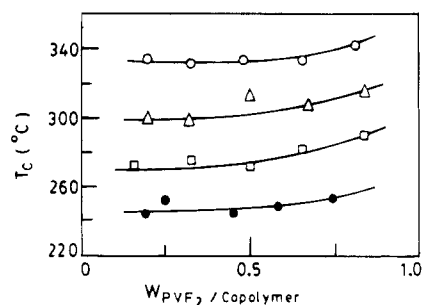


Figure 2. Cloud point curves of PVF₂/PMA and VF₂/VF₄ copolymer/PMA blends: (O) KF/PMA; (Δ) KY/PMA; (□) Cop-1/PMA; (●) Cop-2/PMA.

crystallization temperature to 227 °C without cooling. The peak temperatures were taken as the melting points, and crystallinities were calculated from the peak area using the data station. The instrument was calibrated with indium before use. Representative melting endotherms of PVF₂ are shown in Figure 1. Depending on the crystallization conditions, PVF₂ exhibits three different types of thermograms during melting, containing either single, double, or triple endothermic peaks. These peaks are for different polymorphs of PVF₂: α , γ , and γ' in order of increasing melting points.² The melting characteristics reported here are only for the α phase of PVF₂.

Results

In Figure 2 the LCST phase diagrams of the PVF₂/PMA blends are shown. The cloud point diagrams are very similar to those for PVF₂/PMA blends reported in the literature.²³ From the figure it is clear that the cloud points of the lowest defect content KF PVF₂/PMA blends are higher, and with increasing defect structure in PVF₂, the cloud points of the blends decrease. Here it is necessary to mention that molecular weight decreases in the order KY > KF > Cop-2 > Cop-1; if only the molecular weight factor was operative, the LCST would be in the order Cop-1 > Cop-2 > KF > KY.¹¹ However, from Figure 1 it is apparent that the LCSTs are in the order KF > KY > Cop-1 > Cop-2, and this indicates that here the molecular weight effect is minor compared to the influence of H-H defects present in the PVF₂ chain.

In Figure 3a-c plots of melting point vs crystallinity are shown. From Figure 3a it is clear that at a high level of crystallinity, the melting point increases sharply. This is probably due to thickening of the crystals after completion of primary crystallization. It is more favored for blends of the KFE fraction than those of Kynar

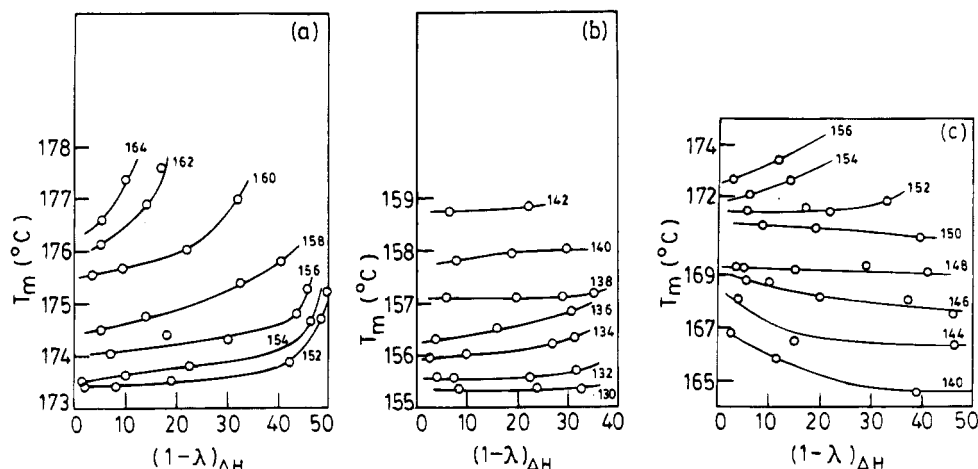


Figure 3. T_m vs crystallinity $(1 - \lambda)_{\Delta H}$ plots of PVF₂ fraction/PMA blends of composition $w_{PVF_2} = 0.75$: (a) KFE/PMA2; (b) KYD/PMA2; (c) KFE/PMA2 at $w_{PVF_2} = 0.50$.

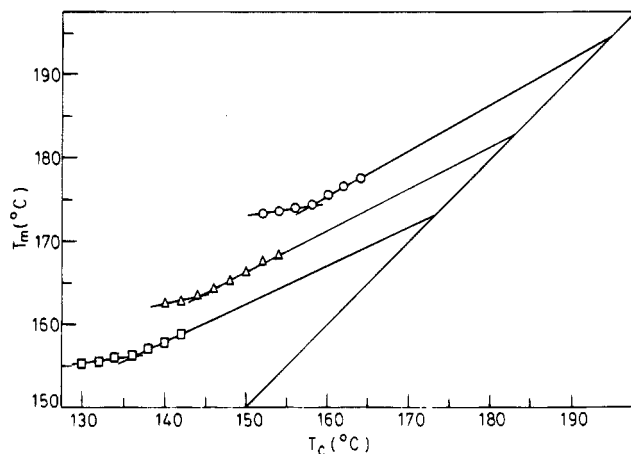


Figure 4. T_m - T_c plots at 10% crystallinity of the α phase of PVF₂ fraction/PMA blends at $w_{PVF_2} = 0.75$: (○) KFE/PMA2; (Δ) KYA/PMA2; (□) KYD/PMA2.

fractions (Figure 3b). In other words, with increasing defect concentration of PVF₂ in the blends, thickening decreases, and this is very similar to the behavior for the pure PVF₂ fractions reported earlier.¹⁹ A comparison of Figures 3a and 3c clearly indicates that thickening is almost negligible in the latter case, and in some cases of Figure 3c, a decrease of T_m with crystallinity occurs. Thus it is quite evident that thickening gradually decreases with increasing PMA content of the blend, but the cause of the decrease of T_m with crystallinity in some cases is still uncertain. The reason for the decrease of thickening with composition of the blend is that thickening is a diffusion-controlled process and with increasingly higher T_g content PMA ($T_g = 10$ °C) in the blend, the diffusion is less favored.

In the T_m - T_c plots of Figure 4 the melting points for 10% crystallinity of the α phase of PVF₂ have been taken at each temperature. The increase of T_m with T_c is slow in the lower T_c region compared to that in the higher T_c region. This causes a break in each case of the PVF₂ blends and is identical to the behavior of the pure PVF₂ fractions.¹⁹ Such behavior is common to many polymers as well.^{20,24,25} The slopes of the T_m - T_c lines after the break are 0.56, 0.52, and 0.45 for the KFE, KYA, and KYD blends, respectively, and are much closer to the theoretical value of 0.50.^{17,24,26} The T_m - T_c plots for the same time of crystallization (12 h) are shown in Figure 5. It is clear from the figure that the break found in the plots of Figure 5 is no longer present

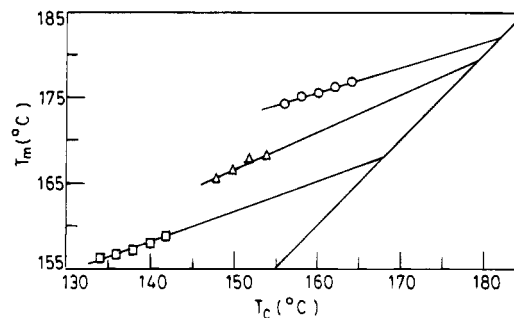


Figure 5. T_m - T_c plots for the same time of crystallization (12 h) for the α phase of PVF₂ fraction/PMA blends: (○) KFE/PMA2; (Δ) KYA/PMA2; (□) KYD/PMA2.

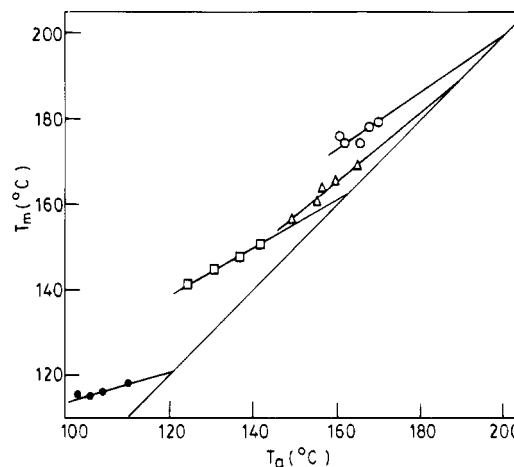


Figure 6. T_m - T_a plots of PVF₂ (whole)/PMA blends at blend composition $w_{PVF_2} = 0.75$: (○) KF/PMA; (Δ) KY/PMA; (□) Cop-1/PMA; (●) Cop-3/PMA.

and the extrapolated T_m^0 values are much lower than those in the former case. The slope values are 0.33, 0.40, and 0.46 for KFE, KYA, and KYD, respectively, and are lower than the theoretical value of 0.5. The reason is the same as for the pure fractions.¹⁹ In Figure 6 the T_m - T_a plots of PVF₂ (whole) blends at composition $w_{PVF_2} = 0.75$ are presented. The T_m^0 values, obtained from extrapolation of the above plots to the $T_m = T_a$ line, together with the T_m^0 values obtained by other methods are presented in Table 2. From the table it is clear that the T_m^0 values obtained from the T_m - T_a plots are much closer to the T_m - T_c plots based on the same crystallinity level. However, T_m^0 s obtained from T_m - T_c plots for the same time of crystallization are much lower than those

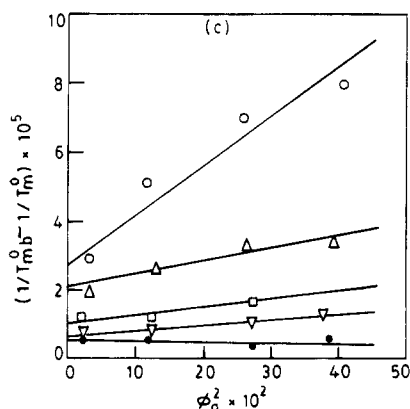
Table 2. T_m° (K), T_{mb}° (K), and Slopes of the Hoffman–Weeks Plots of the PVF₂ (Fraction) Blends Obtained from Different Procedures

fraction	$w_{PVF_2}^a$	$T_m - T_c$ at 10% crystallinity		$T_m - T_c$ at the same time (12 h)		$T_m - T_a$	
		$T_m^\circ \pm 2$	slope ± 0.03	$T_m^\circ \pm 2$	slope ± 0.03	$T_m^\circ \pm 2$	slope ± 0.03
KFE	1.00	479	0.67	460	0.33	476	0.71
	0.88	473	0.60	456	0.32	470	0.70
	0.75	468	0.56	455	0.29	465	0.64
	0.60	463	0.48	454	0.30	461	0.63
	0.47	460	0.44	452	0.31	459	0.58
KYA	1.00	461	0.65	458	0.54	458	0.76
	0.88	458	0.56	454	0.50	454	0.70
	0.73	456	0.50	452	0.45	452	0.71
	0.60	455	0.48	450	0.46	451	0.70
	0.48	455	0.50	449	0.40	451	0.77
KYD	1.00	449 ^b		449	0.38	452	0.67
	0.90	448	0.52	442	0.39	450	0.71
	0.74	447	0.47	441	0.35	450	0.71
	0.59	446	0.47	440	0.37	449	0.76
	0.48	445	0.51	437	0.40		

^a w_{PVF_2} = weight fraction of PVF₂ in the blend. ^b Taken from ref 19.

Table 3. χ_{12} of PVF₂–PMA Blends for Different H–H Defect Content PVF₂ Samples

PVF ₂	H–H defect (mol %)	χ_{12} from T_m° of $T_m - T_c$ plots		χ_{12} from T_m° of $T_m - T_a$ plot
		10% crystallinity	same time (12 h)	
KFE	3.75	-0.267 ± 0.002	-0.081 ± 0.001	-0.221 ± 0.002
KYA	5.06	-0.068 ± 0.001	-0.119 ± 0.001	-0.066 ± 0.001
KYD	5.64	-0.051 ± 0.001	-0.136 ± 0.001	-0.035 ± 0.001
KF	3.50			-0.153 ± 0.001
KY	5.30			-0.119 ± 0.001
Cop-1	15.8			-0.026 ± 0.0005
Cop-3	27.6			$+0.005 \pm 0.0005$

**Figure 7.** $1/T_m^\circ - 1/T_m^b$ vs ϕ_a^2 plots of PVF₂/PMA blends from T_m° of the annealing experiment: (○) KFE; (△) KYA; (□) KYD; (▽) Cop-1; (●) Cop-3.

of the other two methods. It was earlier proved by Nakagawa and Ishida²⁷ that the T_m° obtained from extrapolation of the $T_m - T_a$ plot to the $T_m = T_a$ line is equal to that obtained from extrapolation of the $T_m - 1/l$ plot to $l = \alpha$. This clearly indicates that the $T_m - T_c$ plot for the low level of crystallinity and the $T_m - T_a$ plot yield the correct value of T_m° .

The equilibrium melting points determined by the above three procedures were used to calculate χ_{12} following the method of Nishi and Wang.¹² In Figure 7 plots are shown for $1/T_m^\circ - 1/T_m^b$ vs ϕ_a^2 , with T_m° data obtained from the annealing method. The data fit well on a straight line in each case according to the theoretical expectation, and this is also true for the T_m° data obtained at the same crystallinity level and by the same time method. The χ_{12} values were calculated from the slopes of each plot using $V_a = 70.5 \text{ cm}^3/\text{mol}$ and $V_c = 33.3, 34.1, \text{ and } 35.7 \text{ cm}^3/\text{mol}$ for PVF₂, Cop-1, and Cop-3, respectively. $\Delta H_u = 1.6 \text{ kcal/mol}$,²⁷ $\rho_1 = 1.22 \text{ g/cm}^3$,²⁸ and $\rho_2 = 1.92 \text{ and } 1.97 \text{ g/cm}^3$ for PVF₂ and the

copolymers,¹ respectively. The χ_{12} values are presented in Table 3. From the table it is apparent that χ_{12} obtained from T_m° s at the 10% crystallinity level and χ_{12} from T_m° s of the annealing data are close to each other, and in both cases χ_{12} increases with increasing H–H defect concentration of PVF₂. However, the χ_{12} values obtained from T_m° s of the same time crystallization are quite different from the others, and contrary to the earlier results, χ_{12} decreases with increasing H–H defect content of PVF₂. This latter result does not explain the phase diagram of Figure 2, but the former χ_{12} values explain the phase diagrams very well. Therefore, the χ_{12} values obtained from T_m° s on the same time basis are wrong, and the χ_{12} values obtained by this method by other workers are questionable. It is pertinent to mention that the eq 2 employed here to determine χ_{12} is derived from eq 4 of ref 12 by making an approximation that the molecular weights of the polymers are infinite. However, by taking the measured molecular weights (\bar{M}_w) of the polymers and making numerical calculations on the Nishi and Wang equation (eq 4 of ref 12) with the same data presented here, a strong composition dependence of χ_{12} is observed. The χ_{12} value increases with increasing PMA concentration in each blend. These numerical results of χ_{12} also indicate a dependency of the interaction parameter with H–H defects, in conformity with the graphical results presented above.

T_m° of the whole PVF₂ usually corresponds to that of the lowest defect content fraction of the sample in the pure PVF₂.¹⁹ Thus one would expect that χ_{12} of the unfractionated sample will be close to that of its lowest defect content fraction. However, comparing the χ_{12} values (annealed data) of the whole polymers and those of the fractions, no such trend of interaction is observed. This may be due to the fact that in the blend the lowest defect content fraction experiences more interaction with PMA than the other fractions and this hinders its

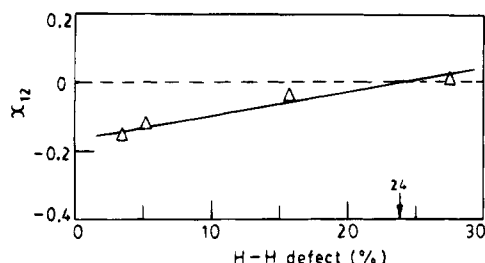


Figure 8. Plots of χ_{12} vs H-H defect concentration of PVF₂/PMA blends obtained from annealing data.

crystallization to yield a higher T_m° as found in the pure PVF₂.¹⁹ The interaction parameter of the whole PVF₂ is, therefore, the "number-average" interaction parameter of various H-H defect content molecules because the interaction energy depends on the numbers of different types of nearest neighboring pairs.²⁹

In Figure 8, χ_{12} values obtained by the annealing method are plotted against the H-H defect concentration of PVF₂ (whole polymer). The dotted line in the figure represents $\chi_{12} = 0$, and we can conclude that PVF₂ samples having a defect concentration below the cross-over point of the $\chi_{12} = 0$ line are miscible with PMA. The χ_{12}^c calculated from eq 3 is 0.0005 for the Cop-3/PMA system. The measured χ_{12} value (0.005) of this pair is higher than χ_{12}^c and, therefore, it should not be miscible. In conformity with this prediction, we obtained turbid films of PMA/Cop-3 at all compositions when cast from DMF solutions. The turbidity of the films increases when they are heated. This indicates that the polymers are immiscible. This further supports that the χ_{12} values obtained from annealing and from the same level of crystallinity method are accurate and can quantitatively predict the phase behavior of PVF₂-PMA blends. Therefore, from Figure 8 we can safely conclude that PVF₂ with a H-H defect level greater than 24 mol % is immiscible with PMA.

Discussion

It is pertinent here to compare these results with those reported in the literature⁷ from the apparent melting point data. There, the apparent melting point-composition plot has a higher slope for KY-PMA blends compared to that of KF-PMA blends. The higher slope was attributed to the greater interaction of KY-PVF₂ with PMA than that of lower defect content KF-PVF₂ assuming that the slopes of the apparent melting point-composition diagrams reflect the interaction of the two polymers in a qualitative way, as many authors have.^{5,30} However, this is not found to be true as justified from the apparent melting point-composition plot for different defect content PVF₂ samples (Figure 9). From the figure it is clear that the KF/PMA and Cop-1/PMA blends have the same slope (28) while the KY/PMA blends have a greater slope (33). The Cop-3/PMA blends have a much lower slope (14). This anomaly is probably due to complications arising from (i) morphological variation with composition of the blends and also (ii) lamellar reorganization.¹⁸ Thus the use of the apparent melting point to predict/compare the nature of a blend is practically impossible. Furthermore, the slower crystallization rate of KY-PVF₂ than that of KF-PVF₂ in the blend⁷ is not due to its greater interaction with PMA as reported in ref 7 but is due to the slower "kinetic immiscibility"³¹ of the KY-PVF₂ system.³²

The present results correctly predict that with increasing H-H defect concentration, or incorporation of

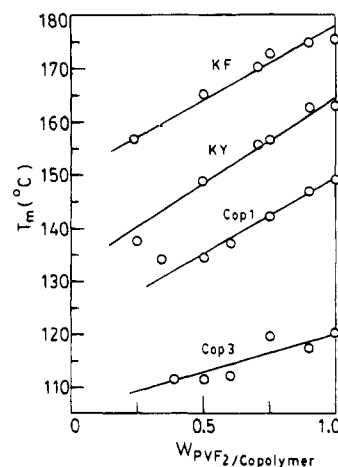


Figure 9. Plots of apparent melting points (T_m) of the blends vs W_{PVF_2} for the indicated PVF₂ samples (samples were crystallized at 25 °C for 24 h and melted at the rate of 40 °C/min to avoid melt recrystallization).

the tetrafluoroethylene unit (pseudo H-H defect), in the PVF₂ chain, compatibility of PVF₂ with PMA decreases. This is because with increasing H-H defect concentration, the dipole moment of PVF₂ decreases by 6–10%.³³ Since the interaction of PVF₂ with polyacrylates is dipolar in nature,³⁴ the interaction with PMA decreases with increasing defect concentration. This inference can also be extended to other polyacrylates or poly(vinyl esters) because the interaction is of the same nature.³⁵

Conclusions

It is established from the above results that caution must be taken in calculating χ_{12} by the melting point depression method. The same and low crystallinity method of obtaining T_m° yields the correct value of χ_{12} . The annealing method of obtaining T_m° also yields the correct value of χ_{12} . However, crystallization for the same time period does not yield an accurate T_m° and hence an accurate χ_{12} . With increasing H-H defect concentration, the blending ability of PVF₂ with poly-(methyl acrylate) decreases, and after 24 mol % H-H defect concentration, it is immiscible with PMA. No conclusion from the apparent melting point depression should be drawn regarding the miscibility of semicrystalline polymers with other polymers.

Acknowledgment. We gratefully acknowledge CSIR, New Delhi, for financial support (Grant No. 4(112)/91 EMRII) of the work.

References and Notes

- (1) Lovinger, A. J. In *Developments in Crystalline Polymers*; Bassett, D. C., Ed.; Applied Science: London, 1981; Vol. 1, p 254.
- (2) Morra, B. S.; Stein, R. S. *J. Polym. Sci., Polym. Phys. Ed.* **1982**, *20*, 2243.
- (3) Briber, R. M.; Khoury, F. *Polymer* **1987**, *28*, 38.
- (4) Alfonso, C. G.; Turturro, A.; Pizzoli, M.; Scandola, M.; Ceccorulli, G. *J. Polym. Sci., Polym. Phys. Ed.* **1989**, *27*, 1195.
- (5) Goh, S. H.; Siow, K. S. *Polym. Bull.* **1988**, *20*, 393.
- (6) Saito, H.; Okada, T.; Hamane, T.; Inoue, T. *Macromolecules* **1991**, *24*, 4446.
- (7) Maiti, P.; Chatterjee, J.; Rana, D.; Nandi, A. K. *Polymer* **1993**, *34*, 4273.
- (8) Huang, J.; Prasad, A.; Marand, H. *Polymer* **1994**, *35*, 1896.
- (9) Cais, R. E.; Solane, N. J. A. *Polymer* **1983**, *24*, 179.
- (10) Flory, P. J. *Trans. Faraday Soc.* **1970**, *7*, 49.
- (11) Olabisi, O.; Robeson, L. M.; Shaw, M. T. *Polymer-Polymer Miscibility*; Academic Press: New York, 1979.
- (12) Nishi, T.; Wang, T. T. *Macromolecules* **1975**, *8*, 909.

- (13) Scott, R. L. *J. Chem. Phys.* **1949**, *17*, 279.
- (14) Patterson, D.; Robard, A. *Macromolecules* **1978**, *11*, 690.
- (15) Runt, J.; Gallagher, K. P. *Polym. Commun.* **1991**, *32*, 180.
- (16) Hoffman, J. D.; Weeks, J. J. *J. Res. Natl. Bur. Stand., Sect A* **1962**, *66*, 13.
- (17) Hoffman, J. D.; Davis, G. T.; Lauritzen, J. I., Jr. In *Treatise on Solid State Chemistry*; Hanay, N. B., Ed.; Plenum Press: New York, 1976; Vol. 3, p 497.
- (18) Rim, P. B.; Runt, J. P. *Macromolecules* **1984**, *17*, 1520.
- (19) Nandi, A. K.; Mandelkern, L. *J. Polym. Sci., Polym. Phys. Ed.* **1991**, *29*, 1287.
- (20) Gopalan, G.; Mandelkern, L. *J. Phys. Chem.* **1967**, *71*, 3833.
- (21) Datta, J.; Nandi, A. K. *Polymer* **1994**, *35*, 4804.
- (22) Rana, D.; Mandal, B. M.; Bhattacharyya, S. N. *Polymer* **1993**, *34*, 1454.
- (23) Bernstein, R. E.; Cruz, C. A.; Paul, D. R.; Barlow, J. W. *Macromolecules* **1977**, *10*, 681.
- (24) Beech, D. R.; Booth, C. J. *J. Polym. Sci.* **1970**, *B8*, 731.
- (25) Cheng, S. Z. D.; Herber, D. P.; Lein, H. S.; Harris, F. W. *J. Polym. Sci.* **1990**, *B28*, 655.
- (26) Mandelkern, L. *Crystallization of Polymers*; McGraw-Hill Book Co.: New York, 1964.
- (27) Nakagawa, K.; Ishida, Y. *J. Polym. Sci., Polym. Phys. Ed.* **1973**, *11*, 2153.
- (28) *Polymer Handbook*, 2nd ed.; Brandrup, J., Immergut, E. H., Eds.; Wiley: New York, 1975.
- (29) Tompa, H. *Polymer Solutions*; Butterworth Scientific: London, 1956; p 70.
- (30) Vion, J. M.; Jerome, R.; Teyssie, P.; Aubin, M.; Prud'homme, R. E. *Macromolecules* **1986**, *19*, 1828.
- (31) The term "kinetic miscibility" is presently used in the case of polyblends by Gvozdic and his co-workers [Prof. N. Gvozdic, MMI, Midland, MI, at the International Symposium of Macromolecules, VSSC, Trivandrum, India]. However, we feel that "kinetic immiscibility" is the most appropriate term in the case of semicrystalline polymer-amorphous polymer blends.
- (32) Maiti, P.; Nandi, A. K., in preparation.
- (33) Lovinger, A. J. *Science* **1983**, *220*, 1115.
- (34) Roerdink, E.; Challa, G. *Polymer* **1980**, *21*, 509.
- (35) Belke, R. E.; Cabasso, I. *Polymer* **1988**, *29*, 1831.

MA950369M